Manganese-doped zinc oxide tetratubes and their photoluminescent properties

Xu, Chunxiang; Sun, Xiaowei; Dong, Zhili; Tan, Swee Tiam; Cui, Yiping; Wang, B. P.

2005

Xu, C., Sun, X., Dong, Z. L., Tan, S. T., Cui, Y. P. & Wang, B. P. (2005). Manganese-doped zinc oxide tetratubes and their photoluminescent properties. Journal of applied physics, 98.

https://hdl.handle.net/10356/99685

https://doi.org/10.1063/1.2138804

Manganese-doped zinc oxide tetratubes and their photoluminescent properties

C. X. Xu and X. W. Sun[a)]
School of Electric and Electronic Engineering, Nanyang Technological University, Nanyang Avenue, Singapore 639798, Singapore and Department of Electronic Engineering, Southeast University, Nanjing 210096, People's Republic of China

Z. L. Dong
School of Materials Science and Engineering, Nanyang Technological University, Nanyang Avenue, Singapore 639798, Singapore

S. T. Tan
School of Electric and Electronic Engineering, Nanyang Technological University, Nanyang Avenue, Singapore 639798, Singapore

Y. P. Cui and B. P. Wang
Department of Electronic Engineering, Southeast University, Nanjing 210096, People's Republic of China

(Received 4 August 2005; accepted 24 October 2005; published online 8 December 2005)

Based on vapor-phase transport method, manganese-doped zinc oxide (ZnO:Mn) tetropod whiskers were fabricated. The pods of the ZnO:Mn whiskers show hexagonal hollow shape with multitips at the front. X-ray diffraction and high-resolution transmission electron microscopy demonstrate that the tube pods and the tips are composed of wurtzite ZnO growing along [0001] direction. The generation of the luminescent center in ZnO whiskers and electron transport between the ground state and the excitation states of Mn^{2+} are analyzed by Raman-scattering, photoluminescence, and photoluminescent excitation measurements. © *2005 American Institute of Physics*.
[DOI: 10.1063/1.2138804]

I. INTRODUCTION

In recent years, nanostructural zinc oxide (ZnO) has attracted great interests because of its potential applications in optoelectronic nanodevices, such as ultraviolet (UV) light-emitting diodes, laser, field emitter, transistors, and sensors, based on the direct wide band gap and large excitonic binding energy. So far, various ZnO nanostructures, such as nanowires,[1] nanobelts,[2] nanopencil,[3] and nanorings,[4] have been fabricated. Some also reported nanotubes[5,6] and tetrapod whiskers[7,8] of ZnO. In this paper, we shall present a tetrapod structure of ZnO with hollow pods and multitips that might be advantageous for gas adsorption, storage, and sensing, employing a vapor-phase transport method. This morphology has not been reported previously.

Besides the attractive applications of ZnO in photonics, some have also paid considerable attentions on ZnO-based diluted magnetic semiconductors (DMSs) realized through transition-metal doping.[9] It has been predicted, from theoretical simulations,[10] that the Mn-doped ZnO (ZnO:Mn) would have such a high Curie temperature that ferromagnetism could be obtained at room temperature. Thus, ZnO-based DMS would have great potential in spintronic devices, such as spin field-effect transistors and quantum computers. Recently, many researchers have reported the optical, electrical, and magnetic properties of ZnO:Mn thin films.[11–15] Low dimension structures would be beneficial in making use of the advantages offered by the spin, in exploring the effect of quantum tunneling of magnetization, and in integrating the DMS with the modern electronic techniques. However, the investigation on nanostructural DMS is insufficient, although a few researchers have synthesized various nanostructures successfully and reported the magnetic behaviors of Mn-doped nanoparticles.[16–19] Additionally, it is very important to understand the transfer process of the charge carriers in DMS materials, however, the mechanism of the ZnO:Mn ferromagnetism is unclear yet. Very recently, ZnO:Mn nanobelts and nanotetrapods were fabricated and characterized.[20,21]

On the other hand, Mn^{2+} acts as an efficient luminescent center in ZnS-based phosphor for photoluminescence and electroluminescence.[22,23] Considering the similarity between ZnS:Mn and ZnO:Mn, the latter was expected to have a good luminescent performance. However, some reports demonstrated a strong quenching action of Mn^{2+} in ZnO host.[21,24] In this paper, manganese is doped into tetratube ZnO. The excitation and recombination processes and host-guest interaction between ZnO and doped Mn^{2+} will be discussed through spectroscopic analysis, which is not only beneficial to understand excitation process of Mn^{2+} emission in ZnO, but also beneficial to explore the electronic transport process in DMS materials.

II. EXPERIMENT

In our previous works, vapor-phase transport (VPT) has been employed to fabricate various nanostructural ZnO, such as nanofibers,[25] nanocombs,[26] nanopins,[27] nanonetworks,[28] and nanodisks.[29] In this paper, a similar VPT process was conducted to prepare tetratubes with multitips by adding

[a)]Author to whom correspondence should be addressed; electronic mail: exwsun@ntu.edu.sg

5 at. % manganese oxide (MnO) into the source mixture of ZnO and graphite powders. Briefly, the source materials were placed at the end of a slender one-end sealed quartz tube in a tube furnace heated at 1100 °C. The substrate used was [100] oriented silicon wafer coated with a thin layer of copper as catalyst. The substrate temperature for growing tetratube structure was about 900 °C.

Scanning electron microscopy (SEM) was employed to examine the morphology of the product. The crystal structure of the sample was characterized by x-ray diffraction (XRD) using Cu $K\alpha$ radiation. The Raman-scattering spectrum was measured by a Renishaw Ramanscope under the excitation of an argon laser operating at 514.5 nm. A JEOL 3010 high-resolution transmission electron microscope (HRTEM) operated at 300 kV was employed to detect the lattice structure. The photoluminescent excitation (PLE) and emission (PL) spectra were measured using a xenon lamp as light source at room temperature.

III. RESULTS AND DISCUSSION

A. Microstructure and growth process

Figure 1(a) shows the SEM and HRTEM images of the product. It can be seen that the product shows a tetrapod structure with one leg missing. Although tetrapod structure is not uncommon, previously reported tetrapods are composed of nanorods or sharp pods.[7,8] In the present case, each pod of the tetrapod morphology shows hexagonal tube structure with multitips at the front of the tubes. As an enlarged SEM image of Fig. 1(a), it can be seen from Fig. 1(b) that the diameter of the hexagonal tubes is about several microns and the thickness of the wall is about 100 nm. It is also noted that several nanorods grow in the hollow tube. This hollow structure should be helpful to adsorbed gases and to capture nanoparticles and biomolecules. Figures 1(c) and 1(d) show the HRTEM of the surface of the tube wall and the corresponding selected area electron-diffraction (SAED) pattern, respectively. The measured d spacing of 0.26 nm along the tube corresponds to the interplanar spacing of (0002). It was found that the tips at the front of tubes and the nanorods in the hollows present the same HRTEM images. This indicates that all the pods of the tetrapod structure grow along the c direction.

Figure 2 shows the XRD pattern of the tetratubes. All diffraction peaks, as indexed in the spectrum, originated from wurtzite structural ZnO with the lattice constants of $a=0.325$ nm and $c=0.5207$ nm. No diffraction peak was found from manganese compound although MnO was mixed into the source materials. Further measurement by energy-dispersive x-ray spectroscopy (EDX) did not show any signal of Mn. This indicates that the content of manganese in the whiskers is too low (<1 at. %) to be detected by XRD and EDX or even no manganese is doped into the product.

Based on the vapor-liquid-solid mechanism, the tetrapod formation should be due to the octahedron nucleation[30] and the hollow tube formation might be due to the evaporation of zinc during the growth process, similar to our previous report on ZnO microtubes.[31] Carbon and its resultant CO play an important role as reducing agents to reduce the high melting

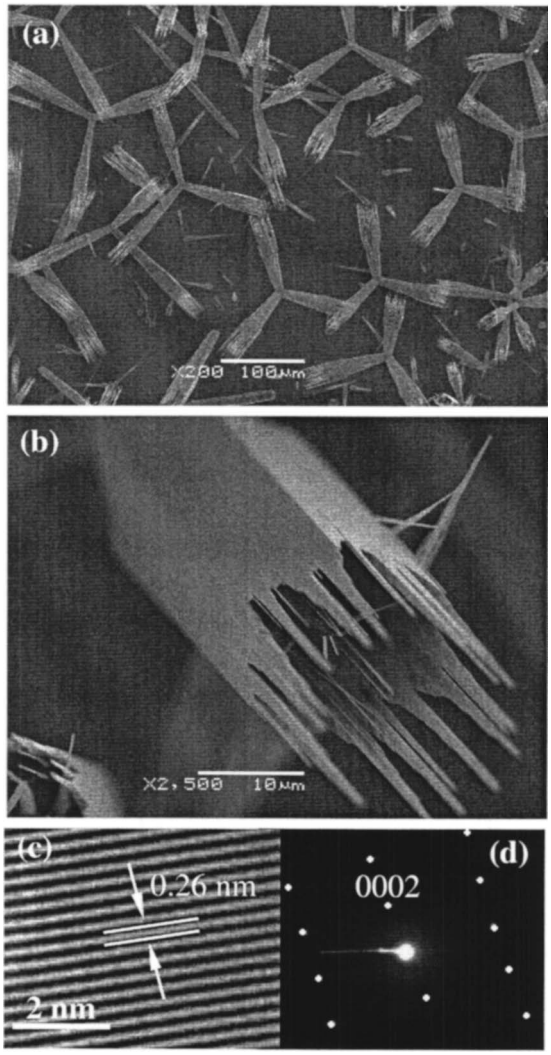

FIG. 1. SEM images of the ZnO:Mn tetrapod structure (a) and an enlarged pod (b) with corresponding HRTEM image (c) and SAED pattern (d).

point ZnO into metal Zn and zinc suboxide (ZnO_x with $x<1$) with low melting point. Similar to gold-assisted vapor-phase transport method,[1] the metal Cu acts as catalyst during the nanostructure formation. The Zn and ZnO_x vapor reacted with the Cu catalyst on the substrate located at the lower-

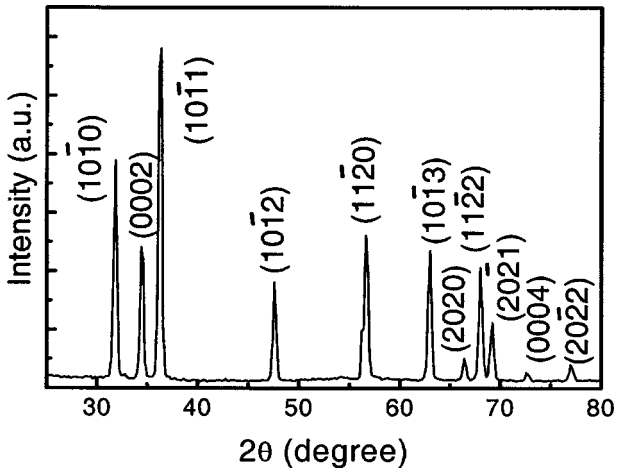

FIG. 2. XRD pattern of ZnO:Mn tetratubes.

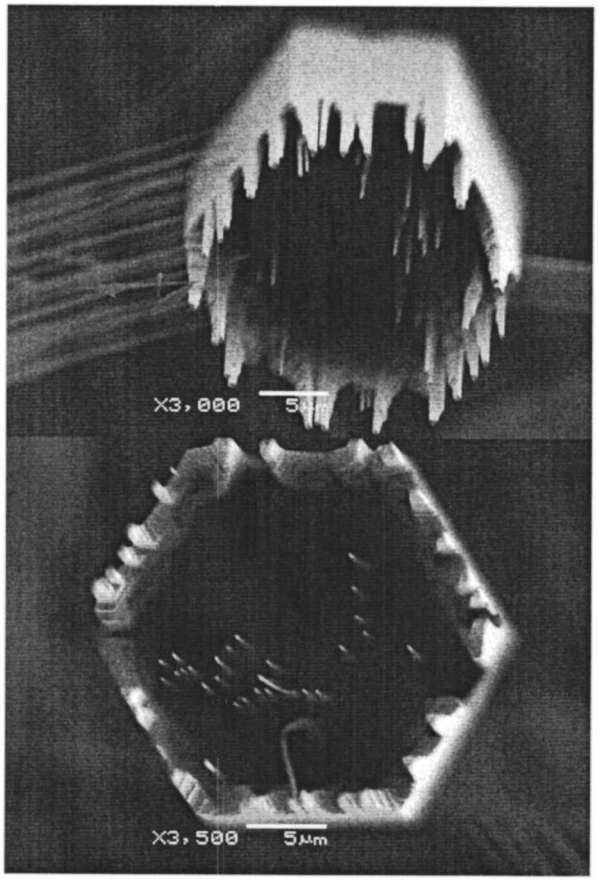

FIG. 3. SEM images of individual pod with shallow hole in the initial growth stage.

temperature region to form nanosized Zn–Cu alloy droplets. The condensed droplets are oxidized into ZnO nuclei and further grow up into the observed morphologies.

On the tetropod structure of ZnO, much information have been given in our previous work[30] and other researchers' reports.[7,8] Briefly, the nucleation is based on an octahedron twin model,[32] which demonstrates an octahedral nucleus composed of eight tetrahedron cells. The eight facets of the octahedron arrange alternatively with the positive (0001) ($+c$) and the negative ($000\,\bar{1}$) ($-c$) facets. According to Laudise's argument,[33] the growth velocity of ZnO nanowhisker along [0001] direction is much faster than that along other directions. Thus, the (0001) surface is favorable to absorb zinc vapor. And the metallic Zn vapors are readily condensed on the four facets along the positive [0001] direction, and oxidized into ZnO, which are further epitaxially growing up into tetraleg structure.

The melting points of Zn and ZnO are 419.53 and 1975 °C, respectively, and the boiling point of Zn is 907 °C. So the as-grown product might have a Zn cap on top or even a Zn–ZnO coaxial structure as what have been reported by other researchers.[34] Tubular structure may be formed with the evaporation of Zn cap at the high growth temperature of about 900 °C. Our previous result of element line scanning[31] has demonstrated the internal surface of the ZnO microtubes fabricated by VPT is Zn rich. Figure 3 presents two individual hollow pods with shallow holes, which reflects more

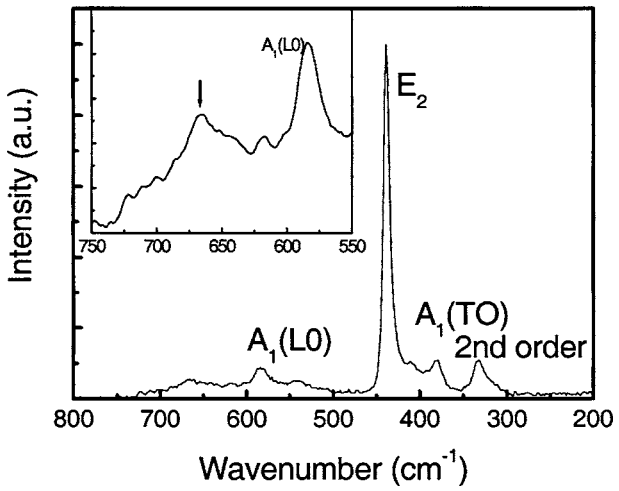

FIG. 4. Raman-scattering spectrum of ZnO:Mn tetratubes inserted with enlarged Mn-related peak. The arrow in the insert indicates the scattering peak of Mn–O vibration.

growth information in the initial growth stage. The hexagonal shallow hole indicates that the tube is formed in the early growth stage due to the zinc evaporation and followed by the epitaxial growth along the tube wall in [0001] direction. The multitips on the front of the wall should be caused by fluctuations of the incoming zinc vapor, roughness of growth front, and growth velocity at different facet on the growth front. It is also clearly seen from Fig. 3 that several nucleus condense in the bottom of the tubular pod and then grow along [0001] direction to form the nanorods in the tubes.

B. Optical properties

The Raman-scattering spectrum of the tetratubes is presented in Fig. 4. According to group theory, the scattering peaks at 437, 380, and 574 cm^{-1}, corresponding to the fundamental optical modes of E_2, A_1 (TO), and A_1 (LO), respectively, should exist in the Raman spectrum of ZnO.[35] The E_2 mode with strongest intensity corresponds to band characteristic of hexagonal wurtzite phase. The weak peaks, A_1 (TO) and A_1 (LO), have been attributed to the intrinsic defects, such as oxygen vacancy and interstitial zinc.[36] The typical Raman spectrum of Fig. 4 indicates the wurtzite structure of the present tetratubes. It is noted that there is a weak peak at about 665 cm^{-1}, as shown in the insert of Fig. 4, which corresponds to the vibration mode of Mn–O.[37] This indicates the existence of the small amount of Mn in the ZnO tetratubes (Fig. 4). In published papers on ZnO:Mn DMS, the concentration of manganese is generally about 5–13 at. %.[11–21] According to the XRD and Raman results, the doped Mn^{2+} in our sample is much lower. It is interesting and noticeable that the magnetism has been observed in ZnO:Mn nanocrystal[38] with 0.2 at. % Mn^{2+}. This implies that our investigation on electron-transport process through the spectral analysis is helpful in understanding the related behaviors as a DMS material.

In order to understand the state of Mn in the ZnO host, PL and PLE processes were investigated. Figure 5(a) shows the normalized PL spectra of the ZnO:Mn tetratubes and the undoped ZnO nanowires fabricated by the same VPT

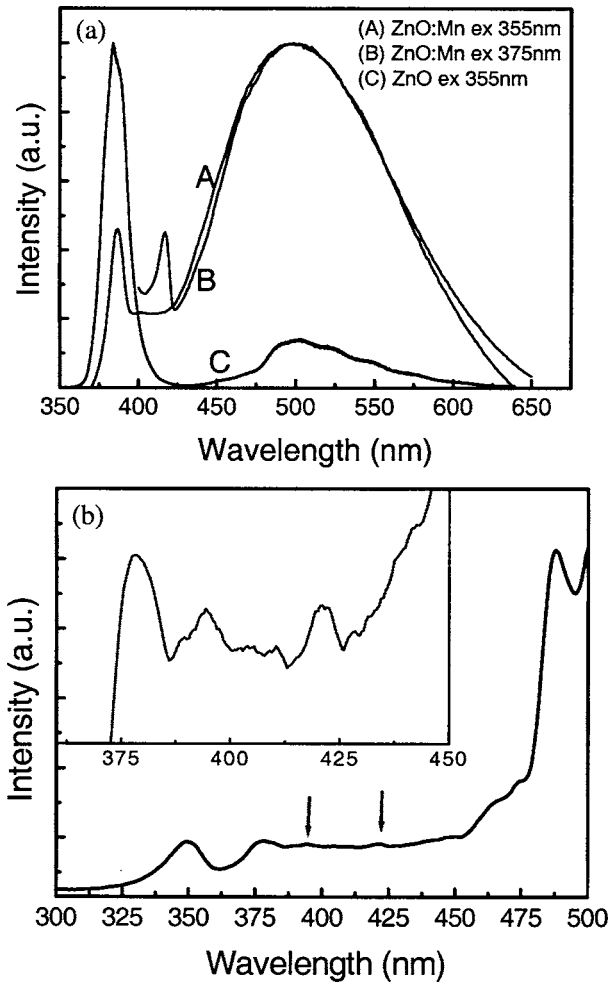

FIG. 5. PL (a) and PLE (b) spectra of ZnO:Mn tetratubes. The curves A, B, and C in (a) correspond to ZnO:Mn, ZnO:Mn, and ZnO samples excited by 355 nm (A), 375 nm (B), and 355 nm (C), respectively. The insert in (b) shows the two enlarged peaks indicated by the arrows.

method. It can be seen that the Mn doping does not change the peak positions in ZnO PL spectrum, which is composed of an ultraviolet band and a green band under the excitation of 355 nm, and is in agreement with other reported results.[39] Compared with the undoped ZnO sample, the intensity of both UV and green bands and the ratio of them reduces after Mn is introduced into the sample. This indicates that the Mn doping increases the nonradiative recombination processes. It is noted that a weak emission peak appears at about 415 nm when the excitation wavelength is selected at 375 nm. It is known that the *d-d* transition of Mn^{2+} is generally forbidden by the selection rule. When the Mn atom is placed substitutionally in a cation site of a $A^{II}B^{VI}$ host lattice, the transition would allowed due to the influence of the crystal field of the host. In order to understand the original of this peak, the PLE spectrum is measured by monitoring the green emission peak [Fig. 5(b)]. As shown in the insert of Fig. 5(b), three weak peaks at 378, 394, and 420 nm, respectively, are observed beside a strong excitation peak at 487 nm. Compared with the reported theoretical and experimental results,[14,15,40] these four excitation peaks can be attributed to the *d-d* transition of Mn^{2+} from the ground state of $^6A_1(S)$ to the excited states of $^4A_1(G)$, $^4E(G)$, $^4T_2(G)$, and $^4T_1(G)$, respectively. The emission peak at 415 nm in Fig. 5(a) can be attributed to the transition from $^4E(G)$ to $^6A_1(S)$ with a Stokes shift of 0.16 eV. This behavior indicates that the manganese atoms are doped into some lattice sites of ZnO. These Mn dopants are electrically activated by participating the above electron and photon transports in the tetratubes. As investigated by Bhargava *et al.*[41] and Norberg *et al.*,[38] the transition threshold of the metal-to-ligand charge transfer (MLCT) lies below the Mn^{2+} $^4T_1(G)$ state in ZnO. This low MLCT level would provide a pathway for nonradiative decay of the excited Mn^{2+} ions.

IV. CONCLUSION

ZnO:Mn tetrastructure was fabricated by Cu-catalyzed VPT method using the mixture of ZnO, MnO, and graphite powders. Each pod of the tetrapod whisker presented hexagonal tube structure with multitips at the front of the tubes grown along [0001] direction. The growth mechanism was interpreted by the VLS process companied by zinc evaporation. The spectral analysis revealed that the manganese atoms were doped into the lattice sites of ZnO and the optical transitions were allowed between the ground state and the excited states of Mn^{2+}. This electron-transport process should also happen in similar materials such as Mn-doped DMS materials. However, our results are of limited importance for understanding Mn-doped ZnO materials due to very low Mn concentration.

ACKNOWLEDGMENTS

The sponsorships from Research Grant Manpower Fund (RG51/01) of Nanyang Technological University and Science and Engineering Research Council Grant (0421010010) from Agency for Science, Technology, and Research (A^*STAR), Singapore are gratefully acknowledged. One of the authors (C.X.X.) would like to acknowledge the financial supports from the National Natural Science Foundation of China (60576008) and the Science Foundation of Southeast University (JX0506118).

[1] M. H. Huang *et al.*, Science **292**, 1897 (2001).
[2] P. Gao and Z. L. Wang, J. Phys. Chem. B **106**, 12653 (2002).
[3] R. C. Wang, C. P. Liu, J. L. Huang, S. J. Chen, Y. K. Tseng, and S. C. Kung, Appl. Phys. Lett. **87**, 013110 (2005).
[4] Z. L. Wang, Mater. Today **7**, 26 (June, 2004).
[5] Y. J. Xing *et al.*, Appl. Phys. Lett. **83**, 1689 (2003).
[6] J. Q. Hu, Q. Li, X. M. Meng, C. S. Lee, and S. T. Lee, Chem. Mater. **15**, 305 (2003).
[7] Y. Dai, Y. Zhang, and Z. L. Wang, Solid State Commun. **126**, 629 (2003).
[8] M. Kiatano, T. Hamabe, and S. Maeda, J. Cryst. Growth **128**, 1099 (1993).
[9] I. Žutić, J. Fabiant, and S. D. Sarma, Rev. Mod. Phys. **76**, 323 (2004).
[10] T. Dietl, H. Ohno, F. Matsukura, J. Cibert, and D. Ferrand, Science **287**, 1019 (2000).
[11] T. Fukumura, Z. Jin, A. Ohtomo, H. Koinuma, and M. Kawasaki, Appl. Phys. Lett. **75**, 3366 (1999).
[12] K. Ueda, H. Tabata, and T. Kawai, Appl. Phys. Lett. **79**, 988 (2001).
[13] Y. W. Heo *et al.*, Appl. Phys. Lett. **84**, 2292 (2004).
[14] T. Mizokawa, T. Nambu, A. Fujinori, T. Fukumura, and M. Kawasaki, Phys. Rev. B **65**, 085209 (2002).
[15] X. M. Cheng and C. L. Chien, J. Appl. Phys. **93**, 7876 (2003).
[16] L. W. Yang, X. L. Wu, G. S. Huang, T. Qiu, and Y. M. Yang, J. Appl. Phys. **97**, 014308 (2005).

[17]J. Luo, J. K. Liang, Q. L. Liu, F. S. Liu, Y. Zhang, B. J. Sun, and G. H. Rao, J. Appl. Phys. **97**, 086106 (2005).
[18]R. Viswanatha, S. Sapra, S. Sen Gupta, B. Satpati, P. V. Satyam, B. N. Der, and D. D. Sarma, J. Phys. Chem. B **108**, 6303 (2004).
[19]K. R. Kittilstved and D. R. Gamelin, J. Am. Chem. Soc. **127**, 5292 (2005).
[20]C. Ronning, P. X. Gao, Y. Ding, Z. L. Wang, and D. Schwen, Appl. Phys. Lett. **84**, 783 (2004).
[21]R. K. Zheng, H. Liu, X. X. Zheng, V. A. L. Roy, and A. B. Djurišić, Appl. Phys. Lett. **85**, 2598 (2004).
[22]J. Han, A. M. R. Senos, and P. Q. Mantas, Mater. Chem. Phys. **75**, 117 (2002).
[23]Y. Hou, X. Xu, Y. Hua, G. Zhang, X. Chen, Y. Li, and Y. Wang, Proceedings of the 8th International Workshop on Inorganic and Organic Electroluminescence, August 1996, Berlin, Germany (Wissenschaft & Technik Verlag, Berlin, Germany 1996), pp. 69–72.
[24]M. Liu, A. H. Kitai, and P. Mascher, J. Lumin. **54**, 35 (1992).
[25]C. X. Xu, X. W. Sun, and B. J. Chen, Appl. Phys. Lett. **84**, 1540 (2004).
[26]C. X. Xu, X. W. Sun, Z. L. Dong, and M. B. Yu, J. Cryst. Growth **270**, 498 (2004).
[27]C. X. Xu and X. W. Sun, Appl. Phys. Lett. **83**, 3806 (2003).
[28]C. X. Xu, X. W. Sun, B. J. Chen, and Z. L. Dong, Appl. Phys. Lett. **86**, 011118 (2005).
[29]X. Xu, X. W. Sun, Z. L. Dong, and M. B. Yu, Appl. Phys. Lett. **85**, 3878 (2004).
[30]C. X. Xu and X. W. Sun, J. Cryst. Growth **277**, 330 (2005).
[31]X. W. Sun, S. F. Yu, C. X. Xu, C. Yuen, B. J. Chen, and S. Li, Jpn. J. Appl. Phys., Part 2 **42**, L1229 (2003).
[32]H. Iwanaga, M. Fujii, and S. Takeuchi, J. Cryst. Growth **183**, 190 (1998).
[33]R. A. Laudise and A. A. Ballman, J. Phys. Chem. **64**, 688 (1960).
[34]J. J. Wu, S. C. Liu, C. T. Wu, K. H. Chen, and L. C. Chen, Appl. Phys. Lett. **81**, 1312 (2001).
[35]M. Koyano, P. QuocBao, L. T. ThanhBinh, L. HongHa, N. NgocLong, and S. I. Katayama, Phys. Status Solidi A **193**, 125 (2002).
[36]J. N. Zeng, J. K. Low, Z. M. Ren, T. Liew, and Y. F. Lu, Appl. Surf. Sci. **197**, 362 (2002).
[37]H. S. Kim and P. C. Stair, J. Phys. Chem. B **108**, 17019 (2004).
[38]X. W. Sun and H. S. Kwok, J. Appl. Phys. **86**, 408 (1999).
[39]Z. W. Jin, Y. Y. Yoo, T. Sekiguchi, and T. Chikyow, Appl. Phys. Lett. **83**, 39 (2003).
[40]N. S. Norberg, K. R. Kittilstved, J. E. Amonette, R. K. Kukkakapu, D. A. Schwartz, and D. R. Gamelin, J. Am. Chem. Soc. **126**, 9387 (2004).
[41]R. N. Bhargava, V. Chhabra, T. Som, A. Ekimiv, and N. Taskar, Phys. Status Solidi B **229**, 673 (2002).